Pulsed Plasma Polymerized Di(ethylene glycol) Monovinyl Ether Coatings for Nonfouling Surfaces

Li-Qiang Chu,* Wolfgang Knoll, and Renate Förch

Max-Planck-Institut für Polymerforschung, Ackermannweg 10, 55128 Mainz, Germany

Received May 24, 2006. Revised Manuscript Received August 13, 2006

BSA and fibrinogen adsorption to ultrathin nonfouling coatings was investigated using surface plasmon resonance spectroscopy. The nonfouling coatings were prepared by pulsed plasma polymerization (pp) of di(ethylene glycol) monovinyl ether (EO2). The pp-EO2 coatings were characterized by X-ray photoelectron spectroscopy and atomic force microscopy. The nonfouling properties of the pp-EO2 coatings were found to correlate with details of the surface chemistry and with the film thickness. BSA and fibrinogen exhibited different adsorption behaviors. We identified the threshold value of the thickness of pp-EO2, above which the films showed excellent antifouling properties. The mechanism by which these films resist protein adsorption is discussed.

Introduction

Prevention of nonspecific protein adsorption continues to be a challenge in the application of polymeric materials in a variety of fields, such as in biomedical devices, membrane separation, and biosensors. Many efforts have thus been put into the modification of polymer surfaces in order to render them resistant against protein adsorption. Surface modification with polyethylene glycol (PEG) (or polylethylene oxide (PEO)) is well-known as an effective method to reduce protein adsorption and cellular adhesion.[1−3] The protein-resistant properties of PEG coating are generally ascribed to steric repulsion effects,[4,5] which originate from the hydrophilicity and flexibility of the PEG chains. This explanation is particularly suitable for those systems with long PEG chains. Previous theoretical and experimental work has shown that the nonfouling performance of PEG coatings is proportional to the length and the density of PEG chains.[4,6,7] On the other hand, the hydration of PEG leads to a layer of tightly bound water molecules around the PEG chain, a so-called shielding layer.[8−11] This water layer is also believed to play an important role in preventing protein adsorption and may explain why densely packed, shorter OEG-SAMs (oligo(ethylene glycol) self-assembled monolayers) also show nonfouling properties.[12−14]

Various strategies for PEG attachment onto surfaces have been investigated, including graft polymerization,[6,15] self-assembly of monolayers (SAM),[14,16,17] and simple adsorption. Physical adsorption has a problem in long-term stability due to detachment, delamination, and desorption. SAM of thiols are limited to only a few substrates, e.g., noble metals such as Au and Ag. Other strategies involve several steps of wet chemical reactions. Recently, several groups[18−26] have demonstrated that plasma polymerization provides a new possibility for achieving nonfouling surfaces. Plasma polymerization of PEO containing molecules resulted in coatings

* To whom correspondence should be addressed. Tel.: (+49) 6131 379324. Fax: (+49) 6131 379100. E-mail: chu@mpip-mainz.mpg.de.

(1) Harris, J. M. *Poly(ethylene glycol) chemistry. Biotechnical and Biomedical Applications*; Plenum Press: New York, 1992.
(2) Kingshott, P.; Griesser, H. J. *Curr. Opin. Solid State Mater. Sci.* **1999**, *4* (4), 403−412.
(3) Castner, D. G.; Ratner, B. D. *Surf. Sci.* **2002**, *500* (1−3), 28−60.
(4) Jeon, S. I.; Lee, J. H.; Andrade, J. D.; Degennes, P. G. *J. Colloid Interface Sci.* **1991**, *142* (1), 149−158.
(5) Jeon, S. I.; Andrade, J. D. *J. Colloid Interface Sci.* **1991**, *142* (1), 159−166.
(6) Kingshott, P.; Thissen, H.; Griesser, H. J. *Biomaterials* **2002**, *23* (9), 2043−2056.
(7) McPherson, T.; Kidane, A.; Szleifer, I.; Park, K. *Langmuir* **1998**, *14* (1), 176−186.
(8) Wang, R. L. C.; Kreuzer, H. J.; Grunze, M. *J. Phys. Chem. B* **1997**, *101* (47), 9767−9773.
(9) Feldman, K.; Hahner, G.; Spencer, N. D.; Harder, P.; Grunze, M. *J. Am. Chem. Soc.* **1999**, *121* (43), 10134−10141.
(10) Pertsin, A. J.; Grunze, M. *Langmuir* **2000**, *16* (23), 8829−8841.
(11) Heuberger, M.; Drobek, T.; Voros, J. *Langmuir* **2004**, *20* (22), 9445−9448.
(12) Harder, P.; Grunze, M.; Dahint, R.; Whitesides, G. M.; Laibinis, P. E. *J. Phys. Chem. B* **1998**, *102* (2), 426−436.
(13) Li, L. Y.; Chen, S. F.; Jiang, S. Y. *Langmuir* **2003**, *19* (7), 2974−2982.
(14) Li, L. Y.; Chen, S. F.; Zheng, J.; Ratner, B. D.; Jiang, S. Y. *J. Phys. Chem. B* **2005**, *109* (7), 2934−2941.
(15) Wang, P.; Tan, K. L.; Kang, E. T. *J. Biomater. Sci. Polym. Ed.* **2000**, *11* (2), 169−186.
(16) Palegrosdemange, C.; Simon, E. S.; Prime, K. L.; Whitesides, G. M. *J. Am. Chem. Soc.* **1991**, *113* (1), 12−20.
(17) Prime, K. L.; Whitesides, G. M. *J. Am. Chem. Soc.* **1993**, *115* (23), 10714−10721.
(18) Beyer, D.; Knoll, W.; Ringsdorf, H.; Wang, J. H.; Timmons, R. B.; Sluka, P. *J. Biomed. Mater. Res.* **1997**, *36*, 181−189.
(19) Mar, M. N.; Ratner, B. D.; Yee, S. S. *Sens. Actuators B* **1999**, *54* (1−2), 125−131.
(20) Wu, Y. L. J.; Timmons, R. B.; Jen, J. S.; Molock, F. E. *Colloids Surf. B* **2000**, *18* (3−4), 235−248.
(21) Zhang, Z.; Menges, B.; Timmons, R. B.; Knoll, W.; Förch, R. *Langmuir* **2003**, *19* (11), 4765−4770.
(22) Johnston, E. E.; Bryers, J. D.; Ratner, B. D. *Langmuir* **2005**, *21* (3), 870−881.
(23) Shen, M. C.; Martinson, L.; Wagner, M. S.; Castner, D. G.; Ratner, B. D.; Horbett, T. A. *J. Biomater. Sci. Polym. Ed.* **2002**, *13* (4), 367−390.
(24) Sardella, E.; Gristina, R.; Ceccone, G.; Gilliland, D.; Papadopoulou-Bouraoui, A.; Rossi, F.; Senesi, G. S.; Detomaso, L.; Favia, P.; d'Agostino, R. *Surf. Coat. Technol.* **2005**, *200* (1−4), 51−57.
(25) Sardella, E.; Gristina, R.; Senesi, G. S.; d'Agostino, R.; Favia, P. *Plasma Processes Polym.* **2004**, *1* (1), 63−72.
(26) Bremmell, K. E.; Kingshott, P.; Ademovic, Z.; Winther-Jensen, B.; Griesser, H. J. *Langmuir* **2006**, *22* (1), 313−318.

10.1021/cm061217g CCC: $33.50 © 2006 American Chemical Society
Published on Web 09/12/2006

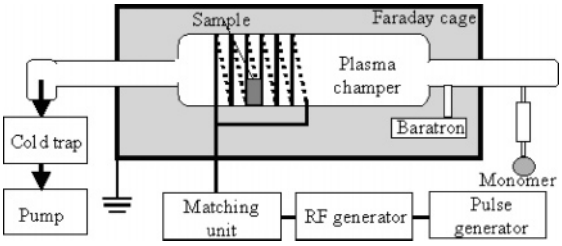

Figure 1. Schematics of the plasma polymerization system.

with abundant PEO, which gave them excellent nonfouling properties.

Plasma polymerization has some advantages for the modification of surfaces. Functional coatings can be obtained easily in a one-step, all dry process. Plasma polymerized thin films are conformal and can be deposited onto a variety of substrates with good adhesion. Ultrathin (d < 10 nm) films can be easily obtained and are potentially promising in the surface modification of nanostructures. Surfaces with nanometer-scale topology can be coated with a thin layer of a functional coating by plasma polymerization, while their morphology would not be significantly altered.

While previously only thicker (d > 30 nm) films were studied,[21] the objective of the present study was to investigate the protein adsorption behavior on a series of plasma polymerized nonfouling films with thicknesses ranging from 1 to 10 nm. Di(ethylene glycol) monovinyl ether (EO2) was used as the monomer in the pulsed plasma polymerization process. BSA and fibrinogen were employed in this work to test nonfouling properties of the deposited pp-EO2 films. Surface plasmon resonance spectroscopy (SPR) is a very sensitive and label-free technique for detection of protein adsorption[21,27,28] and thus was employed in this work. SPR can quantify the protein adsorption in real time with high sensitivity and can be used to estimate the thickness of protein layers adsorbed on the surface by fitting the SPR curve based on Fresnel's equation.

Experimental Section

Materials and Substrates. Di(ethylene glycol) monovinyl ether monomer (98%) and proteins were purchased from Sigma-Aldrich (Germany). The monomer was outgassed three times before use, but was not purified further. The protein solutions were prepared immediately before use by dissolving BSA and fibrinogen into phosphate buffered saline (PBS) solutions at a concentration of 10 wt %. The substrates for the SPR measurements were LaSFN9 glass slides (Hellma Optik, Jena, Germany) coated with approximately 2 nm of Cr and 50 nm of gold, which were thermally evaporated. For the XPS measurements, Si wafers were used as substrates. Mica was used as a substrate for the atomic force microscopy (AFM) measurements since mica provides an atomically flat surface.

Preparation of pp-EO2 Films. Plasma polymerization was carried out in a home-built inductively coupled cylindrical radio frequency (13.56 MHz) plasma reactor (Figure 1). The reaction chamber, enclosed in a Faraday cage, consists of a cylindrical Pyrex tube, 30 cm in length and 10 cm in diameter. The plasma power is generated by a RF generator (Coaxial, RFG150), which passes through a matching network and is delivered to the reactor via a coil placed around the exterior of the reactor tube. A home-built pulse generator is connected to the RF generator to allow pulsing of the radio frequency signal. The plasma can be run either in the continuous wave (CW) mode or in the pulsed mode. The reaction chamber was evacuated using a rotary pump (Leybold Trivac, D16B) and a liquid nitrogen cold trap was used to collect excess organic vapor. A baratron module (MKS, Type 627B) was connected near the inlet to monitor the pressure inside the chamber. Side arms at the reactor inlet allow for the introduction of monomer vapors. The pp-EO2 films were deposited at 20 W with various duty cycles (DCs), i.e., 5/100 and 1/100 ms, respectively. The monomer pressure varied from 0.01 to 0.05 mbar. The deposition time was adjusted to obtain the desired thickness.

Film Analysis. X-ray photoelectron spectroscopy (XPS) was carried out using a Physical Electronics 5600 A instrument. The Mg Kα (1253.6 eV) X-ray source was operated at 300 W. A pass energy of 117.40 eV was used for the survey spectrum. The spectra were recorded using a 45° take-off angle relative to the surface normal.

AFM measurements were carried out using Veeco Dimension 3100 instrument in the tapping mode in ambient air. The surface roughness for an area of 1 × 1 μm^2 was obtained using standard AFM software (Nanoscope 6.11r1).

Protein Adsorption Measured by SPR. The use of SPR for the characterization of thin film has already been discussed in details elsewhere.[29,30] The SPR spectrum, i.e., the reflectivity vs angle curve, can be fitted using Fresnel's equation to obtain the optical thickness ($n*d$) of the dielectric medium. If the refractive index of the thin film is available, one can determine the geometrical thickness of the film. SPR measurements were carried out with a home-built setup, which was based on the Kretschmann configuration.[29] In order to measure protein adsorption in real time, the pp-EO2 sample was attached to a SPR flow cell immediately after plasma polymerization. PBS buffer was introduced into the flow cell in order to stabilize the film. Then protein solution was injected into the cell. The kinetics of protein adsorption can be obtained by monitoring the reflectivity at a fixed angle. After the protein adsorption reached equilibrium, PBS buffer was injected again to rinse the surface. SPR spectra were recorded before and after protein adsorption in order to determine the thickness of adsorbed layer. The refractive index for BSA and fibrinogen used here are 1.45 and 1.39, respectively.[21,31] We present our experimental results for protein adsorption in terms of surface density, which can be calculated using de Feijter's equation:[32]

$$M = d_A \frac{n_A - n_{sol}}{\mathrm{d}n/\mathrm{d}c}$$

Here, d_A is the thickness of the adsorbed layer and dn/dc is the refractive index increment of the molecules. n_A and n_{sol} are the refractive indices of the adsorbed layer and cover media, respectively. For proteins, the dn/dc is equal to approximately 0.182 g/cm^3.[31,32]

Results

Film Analysis. Based on the experience in previous work in this group, 20 W input power and low duty cycles (from 5/100 to 1/100) were employed to ensure that the resulting

(27) Green, R. J.; Davies, J.; Davies, M. C.; Roberts, C. J.; Tendler, S. J. B. *Biomaterials* **1997**, *18* (5), 405−413.
(28) Green, R. J.; Frazier, R. A.; Shakesheff, K. M.; Davies, M. C.; Roberts, C. J.; Tendler, S. J. B. *Biomaterials* **2000**, *21* (18), 1823−1835.
(29) Knoll, W. *Annu. Rev. Phys. Chem.* **1998**, *49*, 569−638.
(30) Knoll, W. *MRS Bull.* **1991**, *16*, 29−39.
(31) Voros, J. *Biophys. J.* **2004**, *87* (1), 553−561.
(32) de Feijter, J. A.; Benjamins, J.; Veer, F. A. *Biopolymers* **1978**, *17*, 1759−1772.

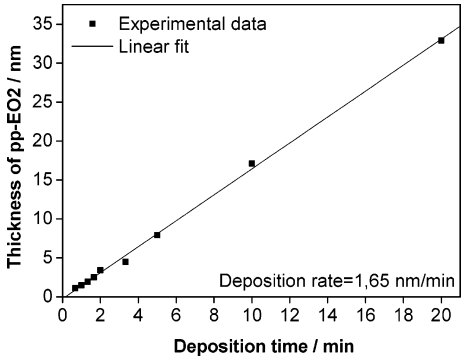

Figure 2. Thickness of pp-EO2 films as a function of the deposition time as determined by SPR measurements. The refractive index of pp-EO2 is $n = 1.451$. Plasma conditions: 20 W, 5/100 ms.

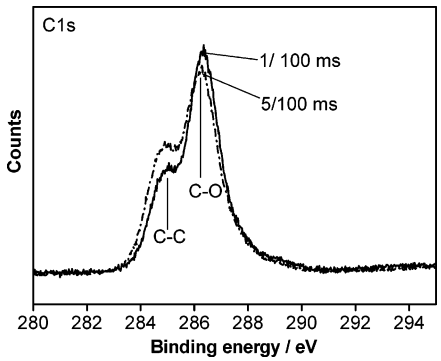

Figure 3. XPS C 1s spectra of pp-EO2 films deposited at different duty cycles (as indicated).

Table 1. Surface Composition from XPS Measurements for a Series of pp-EO2 Films Deposited at Various Duty Cycles[a]

sample	%C	%O	O/C
5/100 ms	69.3	30.7	0.44
1/100 ms	66.5	33.5	0.50
theoretical	66.7	33.3	0.50

[a] Plasma power is 20 W.

pp-EO2 films exhibit good protein resistance for thicknesses larger than 30 nm. The nonfouling properties of these pp-EO2 films were confirmed by SPR experiments (data not shown here). With adjustment of the deposition time, the thickness of pp-EO2 coating can be well-controlled, as shown in Figure 2. The deposition rate was calculated to be 1.65 nm/min.

XPS is a powerful tool to characterize the surface composition of plasma polymerized films. Figure 3 gives the XPS C 1s spectra of the pp-EO2 films deposited at different duty cycles, i.e., 5/100 and 1/100 ms, respectively. The C 1s spectra clearly show two peaks at 285 and 286.5 eV, which can be attributed to C−C and C−O−C functional groups, respectively. It is evident that a high retention of ether groups was achieved at these plasma conditions. As the dc was decreased, the relative C−O−C peak intensity (at 286.5 eV) increased, indicating more ether groups in the deposited films. The retention of ether group can also be confirmed from the O/C as determined from XPS wide scan and summarized in Table 1. The O/C ratio of pp-EO2 deposited at a duty cycle of 5/100 ms is 0.44. If duty cycle is decreased to 1/100 ms, the O/C ratio increased to 0.5, which is the theoretical value for the monomer molecule.

AFM was utilized to study the surface morphology of pp-EO2 films with thicknesses ranging from 2 to 20 nm. The AFM images of the pp-EO2 films with different thicknesses are shown in Figure 4, with mica also being shown as a control. The surface roughness can easily be obtained using standard AFM software. It is found that there is no significant change in surface roughness with increasing film thickness. The roughness of pp-EO2 with less than 3 Å is comparable to that of the bare substrate regardless of the film thickness, indicating that the plasma polymerized films were very flat. It was previously suggested that plasma films only cover the substrate surface completely when thickness $d > 5$ nm, while for very thin films, island formation dominates the process.[33,34] The island formation would however lead to some increase in roughness, which is not observed. Hence, we conclude that already a 2 nm thick pp-EO2 film covers the substrate completely. Additionally, it should be noted that the roughness of 2 nm thick pp-EO2 is 1.9 Å, which is much lower than the film thickness. This also supports the hypothesis that 2 nm thick pp-EO2 already covers the substrate completely. One likely explanation for the present results is that the pp-EO2 films were deposited onto the substrate very slowly and, hence, the plasma film was deposited evenly onto the substrate.

Protein Adsorption. Protein adsorption on the pp-EO2 films was measured in real time using the SPR kinetic mode. The kinetics of BSA and fibrinogen adsorption onto pp-EO2 films of different thickness are given in Figure 5. There is a clear correlation between protein adsorption and the thickness of the pp-EO2 film. With increasing film thickness, the adsorption of both proteins onto the surface decreases and drops to almost zero after rinsing for pp-EO2 film thicknesses exceeding a threshold value. Figure 6 shows the surface density of BSA adsorbed onto pp-EO2 as a function of the film thickness. For BSA and pp-EO2 deposited at dc of 1/100 ms, the threshold value is about 2−3 nm.

In order to test the effect of the pp-EO2 surface chemistry on the BSA adsorption, pp-EO2 deposited at dc's of 5/100 and 1/100 ms, respectively, were compared in Figure 6. Clearly, with decreasing dc, less BSA adsorption was observed for pp-EO2 film with identical thickness.

The adsorption of a larger protein, i.e., fibrinogen, onto the pp-EO2 films of different thicknesses is given in Figure 7. As the pp-EO2 thickness increased, less fibrinogen adsorbed to the surface. It can be noticed that pp-EO2 prepared at dc of 5/100 ms cannot resist fibrinogen adsorption completely in the present thickness range. For the surface prepared at 1/100 ms, 5−6 nm would be required to resist fibrinogen adsorption. Consequently, it appears that the duty cycle employed has a strong influence on the fibrinogen adsorption behavior.

Figure 8 shows a comparison of BSA and fibrinogen adsorption onto pp-EO2 films deposited at a dc of 1/100 ms. The adsorption of both proteins on bare Au is also given as a reference. The amount of BSA adsorbed on bare Au is

(33) Jacobsen, V.; Menges, B.; Scheller, A.; Förch, R.; Mittler, S.; Knoll, W. *Surf. Coat. Technol.* **2001**, *142−144*, 1105−1108.
(34) Jacobsen, V.; Menges, B.; Förch, R.; Mittler, S.; Knoll, W. *Thin Solid Films* **2002**, *409*, 185−193.

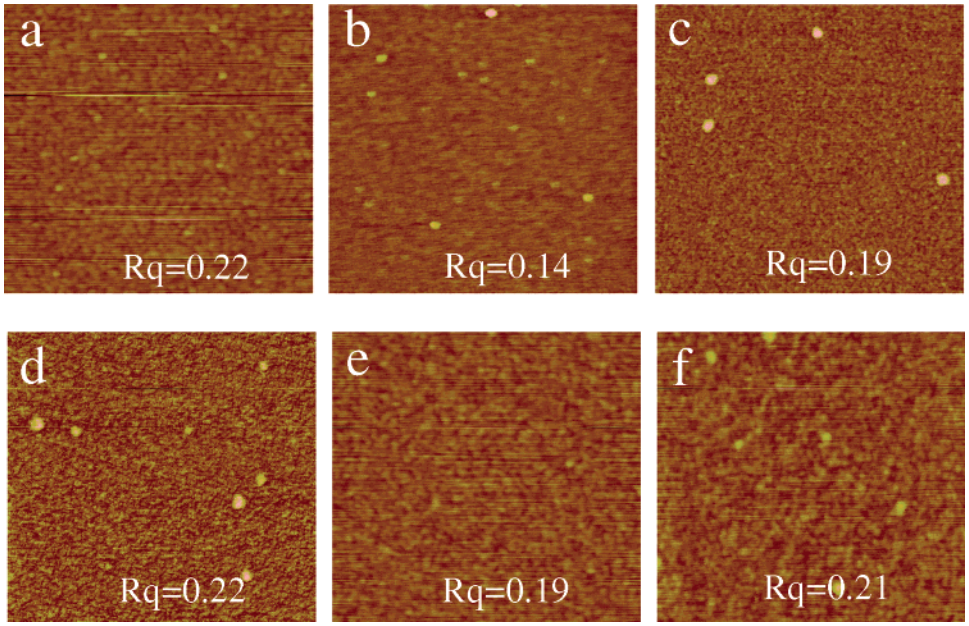

Figure 4. Tapping mode AFM images of pp-EO2 films with increasing thickness taken in ambient air: (a) bare mica as control; (b) 1.7 nm; (c) 3.4 nm; (d) 7.9 nm; (e) 17.1 nm; (f) 32.9 nm. The scan area is 1 × 1 μm^2 in each case. The thickness of the pp-EO2 films was measured by SPR. Plasma conditions: 20 W, 5/100 ms.

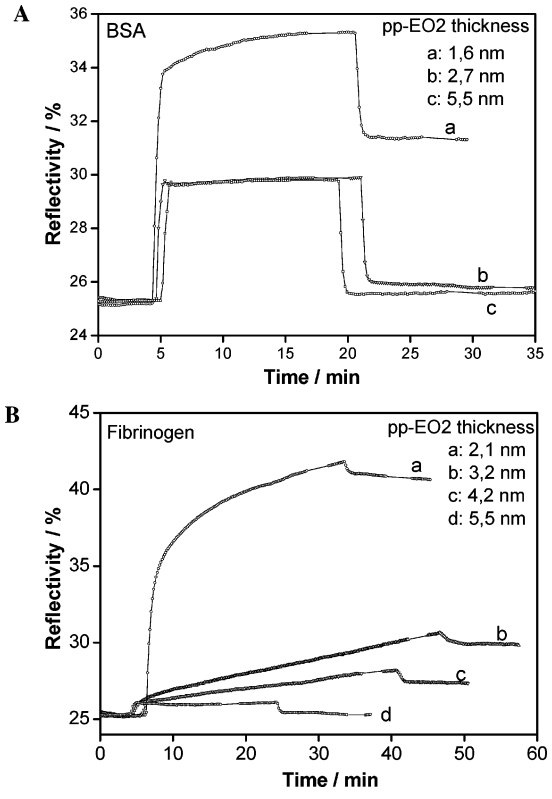

Figure 5. Kinetics of protein adsorption on pp-EO2 films with different thicknesses. (A) BSA; (B) fibrinogen. Plasma conditions: 20 W, 1/100 ms.

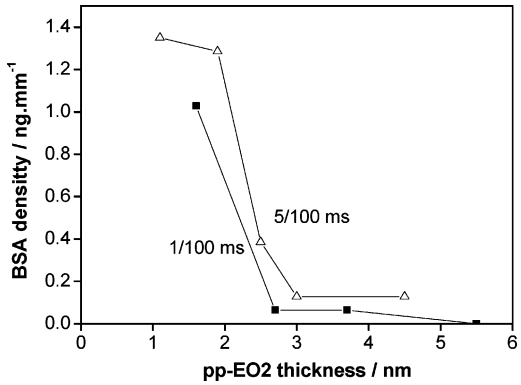

Figure 6. BSA adsorption on pp-EO2 films deposited at different duty cycles.

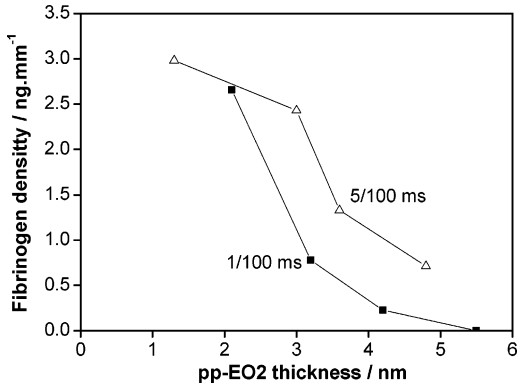

Figure 7. Fibrinogen adsorption on pp-EO2 films deposited at different duty cycles.

calculated to correspond to a surface density of 225 ng/cm^2, which is in agreement with previous reports.[19] From Figure 8, it can be found that thicker pp-EO2 (i.e., ca. 5.5 nm thick) is required to resist fibrinogen adsorption compared to only ca. 2.5 nm for BSA. Additionally, the number of BSA molecules adsorbed on Au is higher than fibrinogen. This result may be related to the size of the proteins: BSA molecules are 68500 Da, which is much lower than fibrinogen molecules with their 340000 Da. It has been documented that protein adsorbed on Au would form a monolayer.[27] On the other hand, after coating Au with a 3 nm thick pp-EO2 film, fibrinogen still adsorbs readily, whereas BSA does not. This indicates that the size of the protein is not the reason for the different behavior of BSA and fibrinogen on a 3 nm

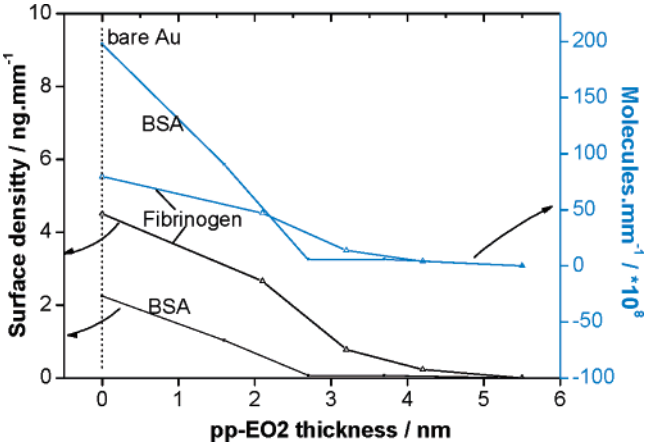

Figure 8. Comparison of BSA and fibrinogen adsorption on pp-EO2 films with increasing thickness. Plasma conditions: 20 W, 1/100 ms.

thick pp-EO2. Vert et al.[35] reported that albumin and PEG are compatible in PBS buffer at room temperature, whereas fibrinogen and PEG are incompatible and show phase separation in solution. They proposed that the compatibility of PEG segments to albumin account for the stealth behavior of PEG bearing molecules or surfaces.

Discussion

Based on the experimental results, it appears that there is a correlation between the pp-EO2 film thickness and its protein resistant properties. A threshold value for pp-EO2 thickness seems to exist, which is approximately 3 nm for BSA and 6 nm for fibrinogen, respectively. Several possibilities may account for this phenomenon.

(1) Defects in the pp-EO2 coatings. If the substrate is not covered completely by thin pp-EO2 coating, proteins may adsorb onto the substrate (Au in the present case) at defect sites.

(2) Diffusion of proteins into the swollen pp-EO2 film. Proteins would diffuse into the pp-EO2 films and approach the underlying substrate, which is active for protein adsorption.

(3) A certain thickness is required because more EO units exist in the thicker pp-EO2 coating. It is possible that only for films with an mount of EO units higher than a threshold value, a water barrier layer, which was regarded as the "functional layer" to resist protein adsorption, can form on the pp-EO2 deposit.

The protein adsorption due to defects should be related to the size of the protein molecules. However, as mentioned in Figure 8, the ability of pp-EO2 films to resist protein adsorption is not size selective. Moreover, our AFM data in Figure 4 suggest a complete coverage of the substrate by a pp-EO2 film of 2 nm thickness. Consequently, we believe that the defect in the thin pp-EO2 film is not the cause for protein adsorption, provided the pp-EO2 coating is thicker than 2 nm.

Protein diffusion through the thin PEG layer has been proposed as an explanation for the protein adsorption on the PEG coating with long PEG graft chains.[15] The swelling of pp-EO2 film may lead to some diffusive pathways for proteins. Our recent results also show that biotin molecules can pass through a 2 nm thick pp-EO2 coating.[36] If the pp-EO2 thickness was increased to 3.5 nm, biotin molecules could not pass through the coating any more. Therefore, for 2 nm and thinner pp-EO2, diffusion of protein or parts of a protein may account for some adsorption. However, this cannot explain why fibrinogen would adsorb onto 4 nm thick pp-EO2 films as shown in Figure 8.

As indicated before, the higher amount of EO units in the low dc pp-EO2 is the reason why BSA and fibrinogen show a reduced protein adsorption deposited at lower duty cycles. The thicker the pp-EO2 coating, the larger the number of EO units. Since the EO units provide a molecular basis for a water barrier layer, the thin pp-EO2 cannot generate a sufficient barrier, in contrast to thicker pp-EO2 films. The density of EO units in the film may also explain why BSA and fibrinogen behave differently with respect to the pp-EO2 surface chemistry and film thickness. Considering the incompatibility of fibrinogen with the PEG segments, more EO units are required to resist fibrinogen adsorption. In contrast, BSA is compatible with PEG and thus requires less EO units.

Conclusions

The aim of this work was to investigate the nonfouling properties of ultrathin pp-EO2 films with thickness lower than 10 nm, providing more insights into the relationship between the structure of pp-EO2 coatings and their ability to resist protein adsorption. XPS results showed that the pp-EO2 deposited at duty cycles of 1/100 ms consisted of a high amount of ether groups. These pp-EO2 coatings show excellent resistance to BSA and fibrinogen provided that their thicknesses are higher than a threshold value. A thicker film of pp-EO2 was required to resist absorption of fibrinogen than of BSA, suggesting that the threshold is not size selective, and the mount of EO units in the pp-EO2 film is of great importance for the protein resistance of surfaces. Plasma polymerization for the fabrication of nonfouling surfaces is particularly promising for large-scale production with good reproducibility as the process is also well-established in industry.

Acknowledgment. We would like to thank Daniela Mössner (IMTEK, University of Freiburg) for the XPS measurements.

CM061217G

(35) Vert, M.; Domurado, D. *J. Biomater. Sci. Polym. Ed.* **2000**, *11* (12), 1307−1317.

(36) Chu, L.; Knoll, W.; Foerch, R. *Plasma Processes Polym.* **2006**, *3* (6−7), 498−505.